The Almost-Magical World of Photonic Crystals

J. D. Joannopoulos
Department of Physics, Massachusetts Institute of Technology, USA

Received July 21, 1995

Within the past few years an exciting new class of materials has emerged which provides capabilities along a new dimension for the control and manipulation of light. These materials, known as "photonic crystals", are viewed ideally as a composite of a periodic array of macroscopic dielectric scatterers in a homogeneous dielectric matrix. A photonic crystal affects the properties of a photon in much the same way that a semiconductor affects the properties of an electron. Consequently, photons in photonic crystals can have band structures, localized defect modes, surface modes, etc. This new ability to mold and guide light leads naturally to many novel applications of these materials as optoelectronic components. An introductory survey including recent exciting developments in the field of photonic crystals is presented.

I. Introduction

The title of this paper was inspired by an article that appeared in Nature magazine[1] a few years ago by Sir John Maddox. It began "If only it were possible to make dielectric materials in which electromagnetic waves cannot propagate at certain frequencies, all kinds of almost-magical things would be possible." Ironically, the article continued in a rather negative tone about the feasibility of such prospects. Nevertheless, during the past five years, there has emerged a new class of materials called Photonic Band Gap Materials or, more simply, Photonic Crystals that appear to provide these almost-magical capabilities. The underlying concept behind these materials stems from early notions by Yablonovitch[2] and John[3]. In a nutshell, the basic idea is to design materials so that they can effect the properties of photons in much the same way that ordinary solids or crystals effect the properties of electrons. Now, the properties of electrons are governed by Schroedinger's equation

$$\left\{-\frac{\nabla^2}{2}+V(\mathbf{r})\right\}\psi(\mathbf{r})=E\psi(\mathbf{r}) \qquad (1)$$

and that of photons by Maxwell's equations, which can be cast in a form that is very reminiscent of the Schroedinger equation,

$$\left\{\nabla\times\frac{1}{\epsilon(\mathbf{r})}\nabla\times\right\}\mathbf{H}(\mathbf{r})=\omega^2\mathbf{H}(\mathbf{r})\ . \qquad (2)$$

Equations (1) and (2) are linear eigenvalue problems whose solutions are determined entirely by the properties of the potential, $V(\mathbf{r})$, or dielectric function, $\epsilon(\mathbf{r})$, respectively. Therefore, if one were to construct a crystal consisting of a periodic array of macroscopic uniform dielectric "atoms," then as in the case of electrons, the photons could be described in terms of a band structure. And if one can have a bandstructure one might be able to have a complete photonic band gap. Defects in the structure could then lead to localized photonic states in the gap, whose shapes and properties would be dictated by the nature of the defect. This ability to confine a photon provides a new "dimension" in ones ability to "mold" or control the properties of light. Therein lies the exciting potential of photonic crystals.

II. The photonic band gap

One appealing aspect of Maxwell's equations, is that, for all practical purposes, they can be solved exactly. With linear materials there are no interactions between photons so that one is left with a fairly standard single-particle problem. This means that theoretical computations can be very helpful, and very useful, working side-by-side with experimental efforts.

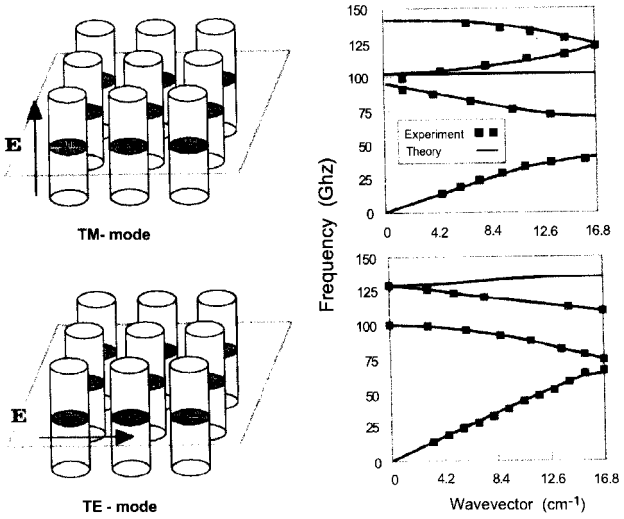

Figure 1. Bandstructures along (10) for the square lattice of alumina rods in air. Comparison of experiment with theory from Robertson et al. [4].

In Fig. 1 we illustrate a comparison between theory and experiment for the dispersion relations of photons in a square lattice of alumina rods ($\epsilon = 8.9$) along the [10] direction by Robertson et al.[4]. For the measurements, 7×25 rods of diameter 0.74 mm were arranged in a square array, as indicated in the insets, with a lattice constant of 1.87 mm. Coherent microwave transient spectroscopy measurements were then performed to measure the frequency and wavevector of the propagating photon. Because of the presence of a mirror symmetry plane, as shown in the insets, the photons decouple into transverse magnetic (TM) and transverse electric (TE) modes. The comparison between experiment and theory is excellent for both the TM and TE modes. We note also that for the TM modes there is an indication of a large photonic band gap between the first and second bands. To determine whether a complete photonic band gap exists one needs to explore all possible directions of propagation. In Fig 2 we show the results of such an exercise for the high-symmetry directions of the Brillouin zone. A complete band gap does indeed exist between the first and the second TM bands. There is, however, no corresponding band gap for the TE modes. It should be possible to explain such a significant fact.

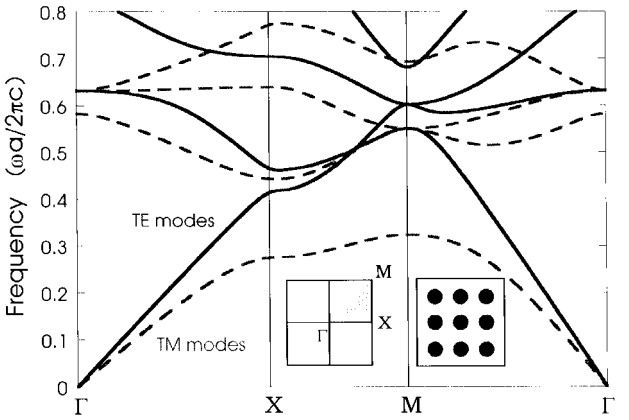

Figure 2. Photonic bandstructure for a square lattice of dielectric ($\epsilon = 8.9$) rods in air with $r = 0.2a$.

If we examine the displacement field pattern associated with the lowest TM band we find that it is strongly concentrated in the dielectric regions. This is in sharp contrast to the field pattern associated with the second TM band which has most of its energy in the air regions. We can quantify these statements by calculating the fraction, f, of electrical energy inside the dielectric regions. For the modes at the X-point, for example, we obtain $f = 0.8$ and $f = 0.3$ for bands 1 and 2, respectively. The first band has most of its power in the dielectric regions and has a low frequency; the second has most of its power in the air region, and has a much higher frequency.

The fractions f for the TE modes do not contrast as strongly. At the X-point, for example, we find $f = 0.2$ and $f = 0.1$ for the first and second bands respectively. In this case, both modes have significant amplitude in the air regions, raising their frequencies. They have no other choice; the field lines must be continuous so they are forced to penetrate the air regions. This is the origin of the small values of f and explains the absence of a band gap for the TE modes. Note that the vector nature of the photon field is central to this argument. The scalar D_z field of the TM modes can be localized within the rods, but the continuous field lines of the TE modes are compelled to penetrate the air regions to connect neighboring rods. As a result, consecutive TE modes do not exhibit markedly different f factors, and band gaps do not appear.

Although we will not discuss it any further here, it is interesting to note that one finds exactly the opposite behavior for TE and TM modes in the case of a crys-

tal with a connected dielectric lattice. The interested reader is referred to Meade et al.[5] for an in-depth discussion of this and other aspects of the nature of the photonic band gap. We shall only state the general rule of thumb: *TM band gaps are favored in a lattice of isolated high-ϵ regions, and TE gaps are favored in a connected lattice.*

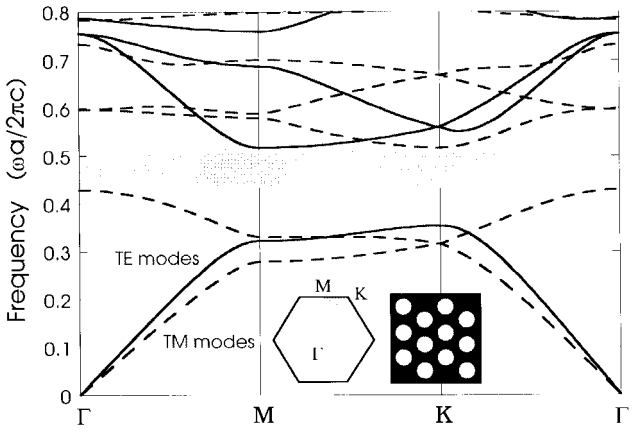

Figure 3. Photonic bandstructure for a triangular lattice of air cylinders ($r = 0.48a$) in dielectric ($\epsilon = 13$).

One can use this rule of thumb to design a photonic crystal that has a gap for both TE and TM modes. The answer is a sort of compromise: we can imagine crystals with high-ϵ regions that are both practically isolated and linked by narrow veins. An example of such a system is the triangular lattice of air columns[6] shown in Fig. 3. A complete photonic band gap clearly exists for both TE and TM polarizations.

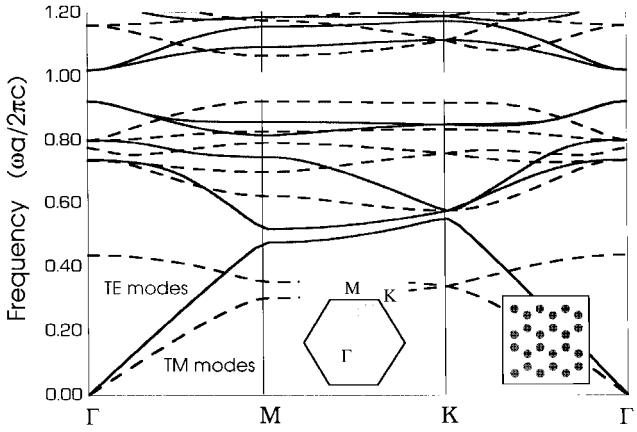

Figure 4. Photonic bandstructure for a honeycomb lattice of dielectric rods in air.

It is also possible to find photonic crystal structures which are not connected, yet exhibit a complete photonic band gap in the higher lying bands. This can occur when there is more than one "dielectric-atom" per lattice constant. An example is the honeycomb lattice of dielectric rods[7] shown in Fig. 4. These types of crystals have the advantage that the larger value of the mid-gap frequency results in a larger value of the minimum feature size. This can be a very important issue when one is concerned with fabrication.

We conclude this section with a rather general observation. It turns out to be quite typical that the bands, above and below a band gap, can be distinguished by where the power lies - in the high-ϵ regions, or in the low-ϵ (usually air) regions. For this reason it is convenient to refer to the band *above* a photonic band gap as the "air band" and the band *below* a gap as the "dielectric band."

III. The waveguide

Once we have a photonic crystal with a gap we can introduce a defect to attempt to trap or localize the light. If we use a *line* defect, we can also *guide* light from one location to another. The basic idea is to carve a waveguide out of an otherwise-perfect photonic crystal. Light that propagates in the waveguide with a frequency within the band gap of the crystal is confined to, and can be directed along, the waveguide. This is a truly novel mechanism for the guiding of light. Traditionally, visible light is guided within dielectric waveguides such as fiber-optic cables, which rely exclusively on total internal reflection. However, if a fiber-optic takes a tight curve, the angle of incidence is too large for total internal reflection to occur, so light escapes at the corners and is lost. Photonic crystals, on the other hand, continue to confine light even around tight corners.

To illustrate these ideas, we turn again to the square lattice of dielectric rods as a simple example and consider only the TM modes. In Fig. 5 we plot the projected bands along the direction of propagation for a waveguide formed by removing one vertical row of rods, as shown in the inset. The shaded regions correspond to states that can propagate through the crystal. The band of states within the gap region corresponds to guided modes, which can travel freely within the narrow waveguide channel. The nature of a guided mode near mid-gap is illustrated in Fig. 6.

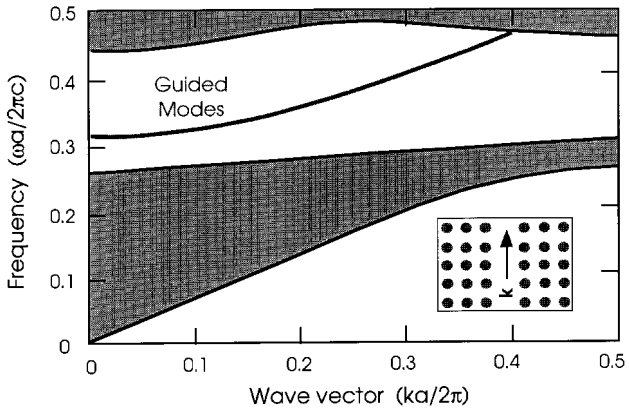

Figure 5. Projected bands for a waveguide in a square lattice of dielectric rods. The waveguide is formed by removing one row of rods as shown in the inset.

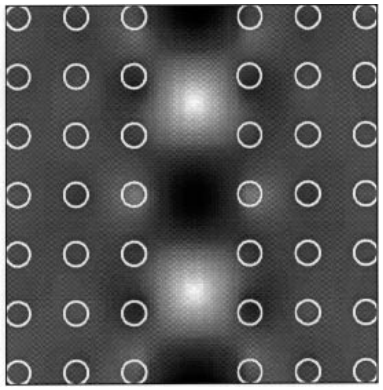

Figure 6. Displacement field of light propagating down a waveguide carved out of a square lattice of dielectric rods.

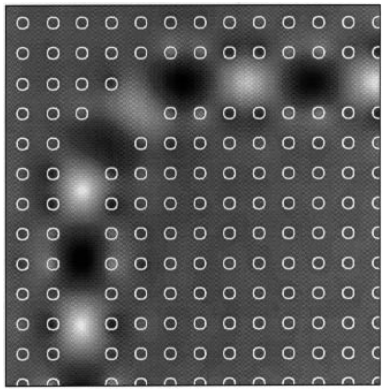

Figure 7. Displacement field of light traveling around a sharp bend in the square lattice of rods.

Once light is induced to travel along the waveguide it really has no where else to go. An intriguing aspect of photonic crystal waveguides is that they provide the only means possible to guide visible light, tractably and efficiently, through narrow channels of *air*. Since the frequency of the guided mode lies within the photonic band gap, the mode is forbidden to escape into the crystal. The primary source of loss can only be reflection back out the waveguide entrance. This suggests that we may use a photonic crystal to guide light around tight corners. This is shown in Fig. 7. Even though the radius of curvature of the bend is less than the wavelength of the light, nearly all the light that goes in one end comes out the other!

Another example of a tight bend in a photonic crystal waveguide is shown in Fig. 8. This is for TE modes propagating around a 60° bend in a triangular lattice of air columns in dielectric. Again, nearly all the light that goes in one end comes out the other.

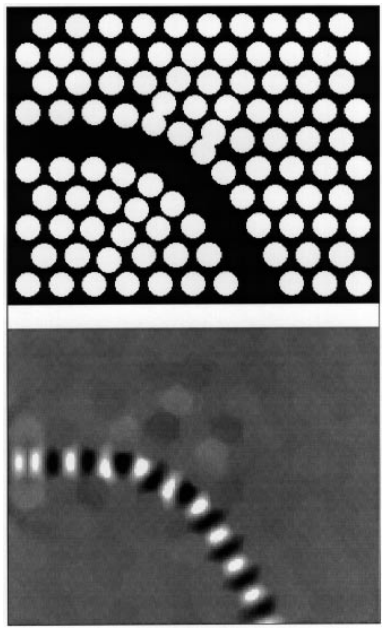

Figure 8. Magnetic field (bottom panel) of light propagating through a waveguide (top panel) formed in the triangular lattice of air cylinders.

IV. The cavity

We can also create imperfections that may trap light at a point within the crystal. One class of imperfections of this type involves changing the dielectric medium in some local region of the crystal, deep within its bulk. As a simple example, consider making a change to a single "dielectric atom" by modifying its dielectric constant, modifying its size, or simply removing it from the crystal. The effect of creating a vacancy in the square lattice of rods is illustrated in Fig. 9. A defect state does indeed appear in the photonic band gap leading to a strongly localized state as shown in the figure. By removing a rod from the lattice, we create a *cavity* which

is effectively surrounded by reflecting walls. It the cavity has the proper size to support a mode in the band gap, then light cannot escape, and we can pin the mode to the defect.

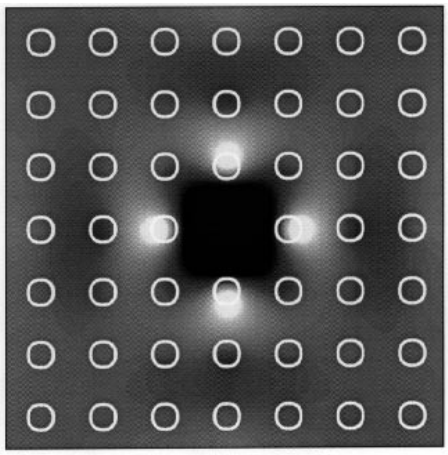

Figure 9. Displacement field for a vacancy in the square lattice of dielectric rods.

If the defect involves removal of dielectric (an "air defect" as in the case of the vacancy) then the cavity mode evolves from the dielectric band and can be made to sweep across the gap by adjusting the amount of dieletric removed. Similarly, if the defect involves the addition of extra dielectric material (a "dielectric-defect") then the cavity mode drops from the air band. The results of this exercise are shown in Fig. 10. In both cases, the defect state can be tuned to lie anywhere in the gap.

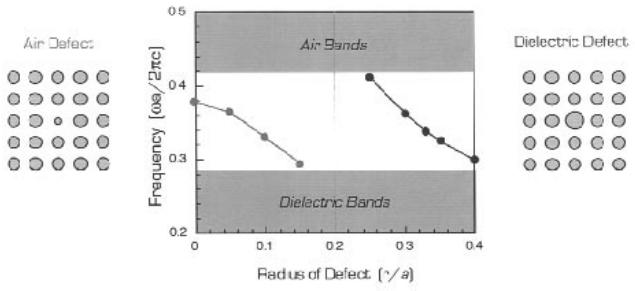

Figure 10. Localized states in the gap for a defect formed by varying the radius of a single rod in the square lattice of dielectric rods. No defect corresponds to $r = 0.2a$.

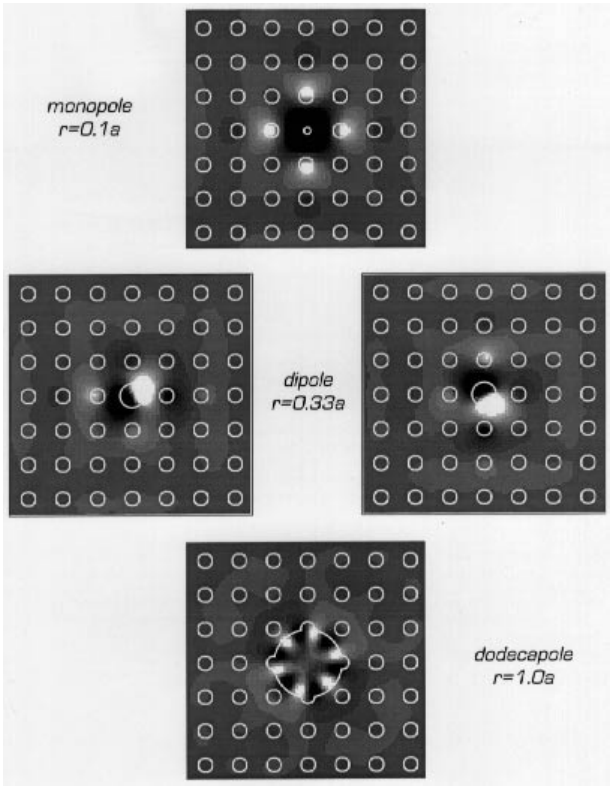

Figure 11. Displacement fields associated with selected defect states as indicated.

Apart from tuning the frequency, one also has some control over the symmetry of the localized photonic state. For example, in Fig. 11 we show the symmetries of the localized photon for three different values of the defect radius. For the case of $r = 1.0a$ we find a field pattern that is very reminiscent of the "whispering gallery" mode observed in microdisk laser cavities. Further information about air- and dielectric-defects can be found in Refs. [8-10].

The flexibility in tuning the properties of defects makes photonic crystals a very attractive medium for the design of novel types of filters, couplers, laser microcavities, etc. [11, 12]. In the case of laser cavities, photonic crystals provide a particularly unique capability - the control of spontaneous emission. This is illustrated in Fig. 12. The rate of spontaneous emission of a given initial state is proportional to the square of a matrix element and the density of final states. In free space, the "natural" rate of emission is proportional to the free-photon density of states per unit volume, D_f, which scales as

$$D_f \sim \frac{1}{\omega} \cdot \frac{1}{\lambda^3}$$

where ω is the frequency of the transition and λ the wavelength of light. If the system is a photonic crystal with a photonic band gap around ω, there are no allowed modes to couple to and spontaneous emission is severely inhibited. Conversely, if the photonic crystal is designed to have a point-defect with a localized, or more generally, a resonant state at ω, then the emission rate could be enhanced dramatically by the increase in the density of final states. An estimate of this enhancement can be obtained from the following simple argument. The density of states per unit volume for the resonance, D_r, will scale as

$$D_r \sim \frac{1}{\Delta\omega} \cdot \frac{1}{V}$$

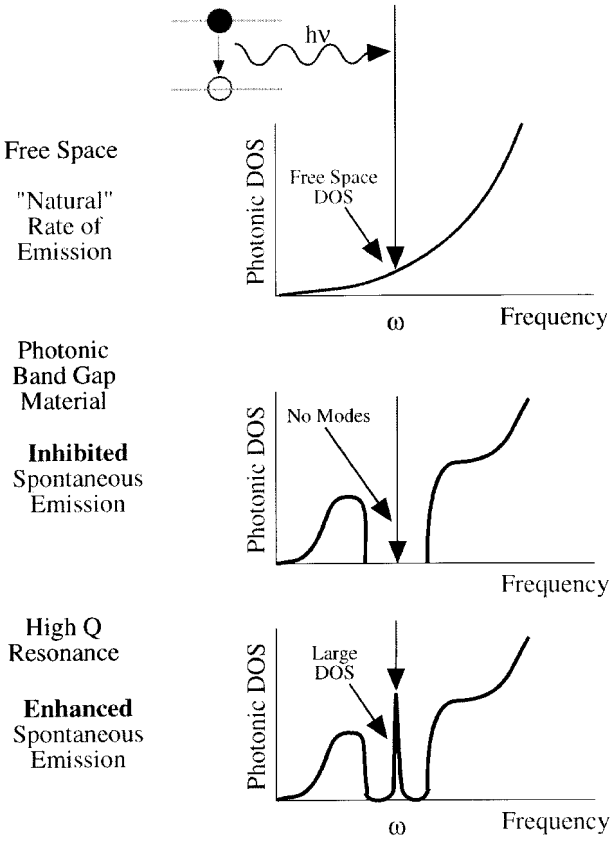

Figure 12. Schematic representation showing the control of spontaneous emission by a photonic crystal as discussed in the text.

where $\Delta\omega$ is the frequency width of the resonance and V is its effective spacial volume. The enhancement factor is then given roughly by

$$\frac{D_r}{D_f} \sim \frac{\omega}{\Delta\omega} \cdot \frac{\lambda^3}{V} = \frac{Q}{(V/\lambda^3)}$$

where $Q \equiv \Delta\omega/\omega$ is the quality factor of the cavity. Thus high Q and small spacial volumes can lead to significant enhancement of spontaneous emission. Since the smallest volume V must be on the order of λ^3, the largest enhancement will be on the order of Q.

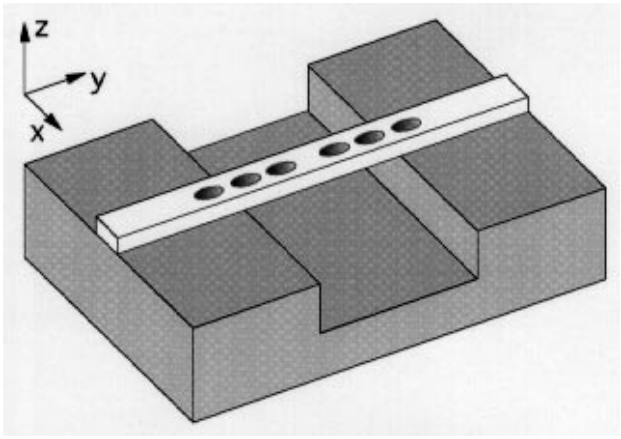

Figure 13. The air-bridge microcavity.

One recent intriguing new design[13] of a laser microcavity involves a high Q, single-mode, bridge configuration as shown in Fig. 13. This design employs a 1D photonic crystal to confine light in the direction along the bridge and near its center, and total internal reflection to confine light in the transverse directions. The defect at the center of the bridge sustains only one cavity mode whose field patterns are illustrated in Fig. 14. The electric field (top panel) is polarized mostly in the plane of the substrate while the magnetic field (bottom panel) is mostly normal to the substrate. The electric field has a nodal point at the center of the cavity. The fields decay rapidly; the modal volume is smaller than half of a cubic half-wavelength. To estimate the Q of this cavity mode, we perform a time-dependent analysis in two-dimensions. The defect structure considered is shown in Fig. 15. We now introduce a pulse into the microcavity and compute the number of optical cycles required for the power to decay by a factor of $e^{-2\pi}$. A more detailed description of this procedure can be found elsewhere[10]. This gives a Q of 1.3×10^4 for this structure. Moreover, we can perform a similar two-dimensional time- dependent analysis to estimate the effects of random disorder at the dielectric-air interfaces. Such disorder will typically arise during fabrication. The amount of disorder will of course depend

on the minimum feature sizes and the fabrication technique. Interestingly, for a structure with surface disorder whose *average* size is as large as 5% of the width of the waveguide, as shown in Fig. 16, the Q is still about 10^4!

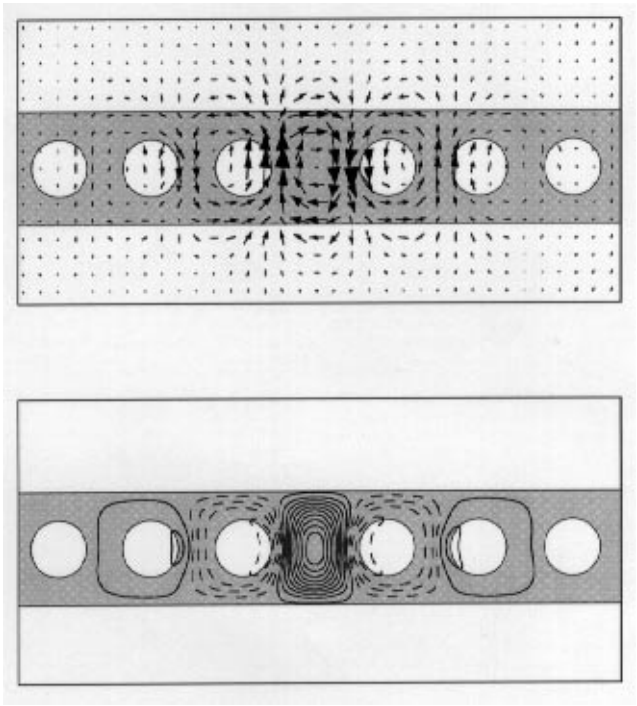

Figure 14. Plots of the electric field (top panel) and magnetic field (bottom panel) in a plane slicing through the middle of the guide for the air-bridge microcavity.

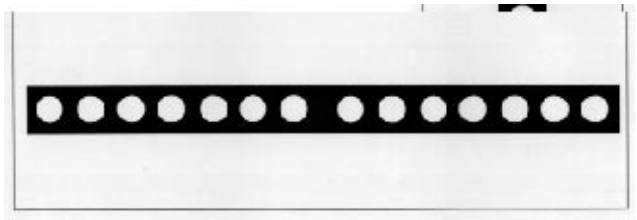

Figure 15. A model of the cross-section of the air-bridge in 2D.

From the field pattern in Fig. 16 we can see why this cavity is rather robust with respect to random defects. First of all, the wavelength of the mode is significantly larger than the characteristic size of the defects. Secondly, most of the energy of the mode is concentrated in the middle of the cavity and away from the surface. This makes the effect of the surface roughness much less significant for this structure than, say, microdiscs in which the high-Q modes propagate along the boundary of the discs.

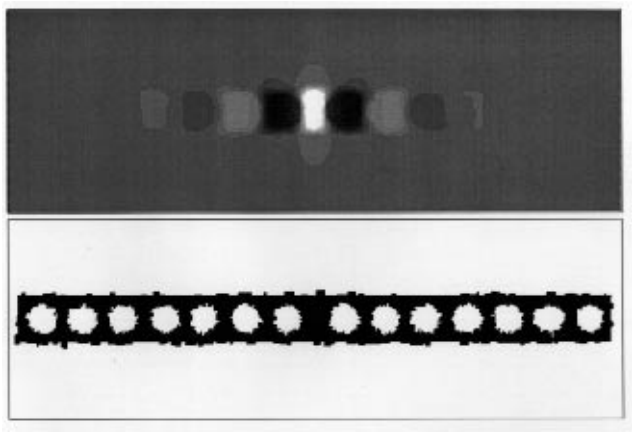

Figure 16. A model of the cross-section of the air-bridge in 2D including the effects of disorder. The magnetic field of the cavity mode is shown in the top panel.

Experimentalists have begun exploring the possibilities of fabricating these microcavities with silicon-based materials and with III-V semiconductor-based materials. Very recently, Professor Kolodziejski's group at MIT has successfully demonstrated the feasibility of building suspended structures with micro-sized features. Of course, submicronsized features will be necessary in order to deal with photons at 1.5microns, which is the canonical frequency of the optoelectronics industry.

V. A 3D photonic crystal for submicron fabrication

In order to have complete control over light we need to employ a 3D photonic crystal. Since Maxwell's equations scale with the size of the system, a photonic crystal designed at one lengthscale will have the same fractional gap as the crystal at any other lengthscale. A given photonic crystal designed to operate at microwave frequencies will have feature sizes on the order of mm's, and at 1.5 microns feature sizes on the submicron lengthscale.

The first photonic crystal possessing a complete gap was fabricated by Yablonovitch in 1991 for the microwave regime[14]. Since then, several other 3D photonic crystal designs have appeared that offer complete photonic band gaps[15–18].

Of these, the Ho et al. structure[17], is the smallest three-dimensional photonic crystal with a complete gap to be manufactured to date. Özbay et al.[19] have used a clever technique of stacking thin micromachined

(110) silicon wafers to fabricate these photonic crystals for wavelengths approaching 600 microns.

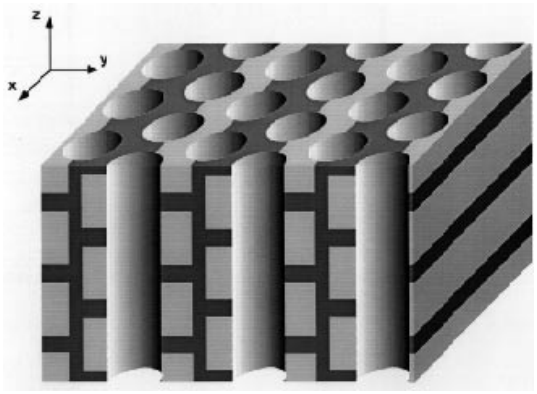

Figure 17. 3D photonic crystal designed to be amenable for submicron fabrication. Dark gray and light gray regions may correspond to Si and SiO_2 respectively. The long cylindrical columns are filled with air.

The ultimate goal, of course, is to design and fabricate photonic crystals for use at 1.5 microns. This is certainly not a trivial task. A new class of photonic crystals, designed specifically to be amenable for fabrication at submicron length scales, has recently been introduced by Fan et al.[20]. One embodiment of this type of photonic crystal is shown in Fig. 17. The crystal is designed to be built in a layered fashion, using two dielectric materials (e.g. Si and SiO_2), with a series of holes etched at normal incidence throu?h the top surface after growth is completed. In order to create a crystal with a larger dielectric contrast, one of the two dielectric materials can be chosen so that it can be removed at the end by selective etching. The sequence of "growth" steps illustrated in Fig. 18 can help the reader visualize the basic elements that make up the crystal structure.

One begins by depositing a layer of Si of thickness d on a substrate of choice and by etching grooves into the Si layers as shown in part (a). The grooves run normal to the page and are separated by a distance a; they have a depth d and a width w. The grooves are then filled with SiO_2. The next step consists in growing another Si layer of height h on top of the previous layer, as shown in part (b), and etching long grooves of depth d and width w into this layer, as shown in part (c). We note that these grooves actually extend into the first layer and are translated by a distance $a/2$ with respect to the first layer. After filling the grooves with SiO_2, another Si layer of height h is deposited on the top surface and long parallel groves are etched. The grooves are translated again by a distance $a/2$ with respect to the previous layer, as shown in part (d). From this point on, the structure repeats itself every two layers. Once this process is completed, an array of long cylindrical holes is etched into the top surface of the structure, at normal incidence. In general, the cross section of the holes can be either circular or elliptical with parameters r_1 and r_2, as shown in part (e).

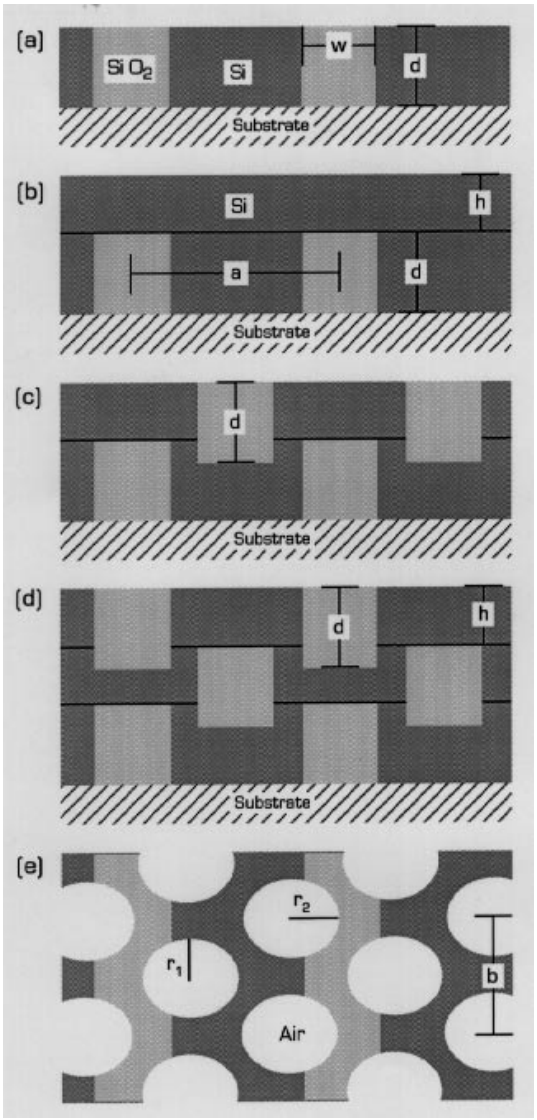

Figure 18. Schematic growth sequence for the structure in Fig. 17. (a) (d) are cross-sectional views, (e) is a plan view.

The design of this structure has many degrees of freedom which can be used to optimize the size of the gap. Using a dielectric constant of 12.096 for Si at 1.53 μm and 2.084 for silica, gives an optimized photonic band gap of about 14%. A very significant improvement can be made by simply removing the oxide. The

resulting photonic crystal structure is illustrated in Fig. 19. With optimized parameters $w = 0.36a$, $d = 0.51a$ and $r/ = r_2 = 0.24a$, one finds a 23% gap as shown in the bandstructure of Fig.20.

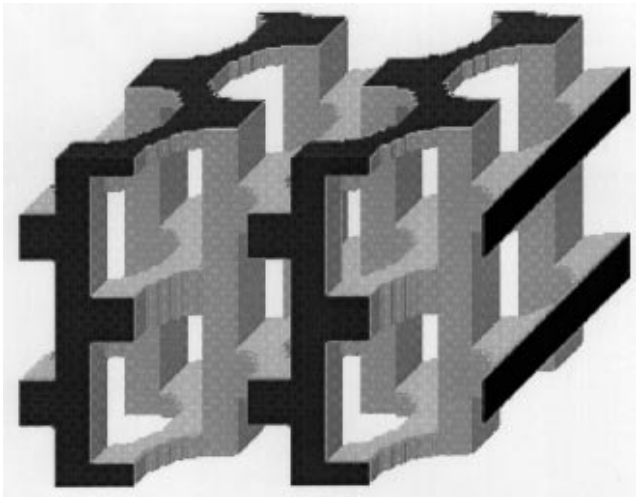

Figure 19. The photonic crystal of Fig. 17 with the SiO_2 removed. The structure consists of a dielectric skeleton of Si embedded in air.

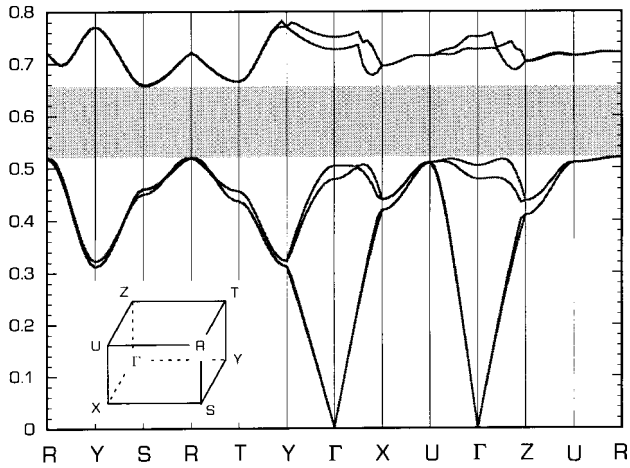

Figure 20. The bandstructure for the photonic crystal of Fig. 19. The shaded region identifies a 23% complete photonic band gap.

Given a 3D photonic crystal with a complete gap as in Fig. 20, one has the possibility of introducing a defect in the structure which will create a localized state in the gap. If this is a point-like defect then the photon mode will be completely localized about a point. In Fig. 21 we show the power associated with an air-defect created by removing a small amount of dielectric from one of the vertical dielectric columns of the crystal structure displayed in Fig. 19. The resulting defect mode has a state near mid gap and is very well localized in a torus-shape whose cross section is plotted in Fig. 21. Of course, as discussed in Section IV, the size of the imperfection can be varied to tune the properties of the defect state.

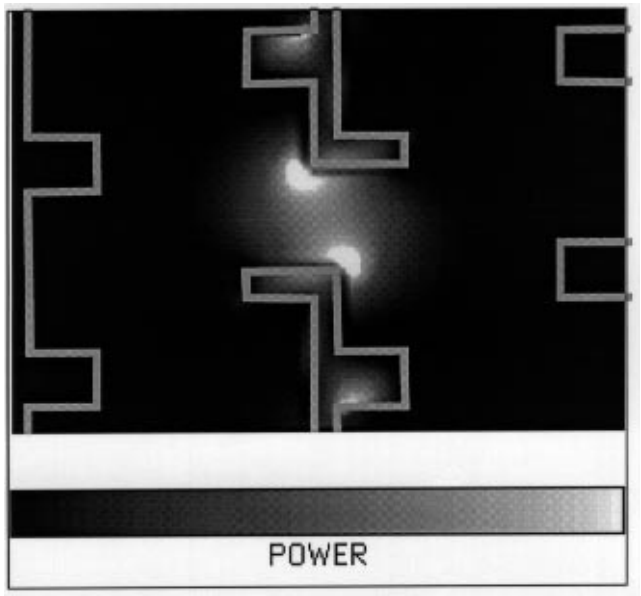

Figure 21. Fig. 21. Power distribution for an air defect in the photonic crystal of Fig. 19, in a $\hat{y} - \hat{z}$ cross-section as shown.

Acknowledgments

The author gratefully acknowledges collaborations and contributions of K. Brommer, J. Chen, S. Fan, I. Kurland, R. Meade, A. Rappe, and P. Villeneuve to all aspects of this work. This work was supported by the MRSEC Program of the NSF under award No. DMR-9400334.

References

1. J. Maddox, Nature, **348**, 481 (1990).
2. E. Yablonovitch, Phys. Rev. Lett. **58**, 2509 (1987).
3. S. John, Phys. Rev. Lett. **58**, 2486 (1987).
4. W. Robertson, G. Arjavalingam, R. Meade, K. Brommer, A. Rappe, and J. Joannopoulos, J. Phys. Rev. Lett. **68**, 2023 (1992).
5. R. Meade, K. Brommer, A. Rappe and J. Joannopoulos, J. Opt. Soc. Am. **10**, 328 (1993).
6. R. Meade, K. Brommer, A. Rappe and J. Joannopoulos, J. Appl. Phys. Lett. **61**, 495 (1992).

7. J. Joannopoulos, R. Meade and J. Winn, *Photonic Crystals,* (Princeton Press, Princeton, N.J, 1991).
8. R. Meade, K. Brommer, A. Rappe and J. Joannopoulos, J. Phys. Rev. B**44**, 13772 (1991).
9. E. Yablonovitch, T. Gmitter, R. Meade, A. Rappe, K. Brommer and J. Joannopoulos, Phys. Rev. Lett. **67**, 3380 (1991).
10. S. Fan, J. Winn, A. Devenyi, J. Chen, R. Meade and J. Joannopoulos, J. Opt. Soc. Am ., (1995) in press.
11. R. Slusher, (1993) Optics and Photonics News Feb., 8.
12. R. Meade, A. Devenyi, J. Joannopoulos, O. Alerhand, D. Smith, and K. Kash, J. Appl. Phys. **75**, 4753 (1994).
13. P. Villeneuve, S. Fan, J. Chen, J. Joannopoulos, K. Lim, G. Petrich, L. Kolodziejski and R. Reif (1995) Appl. Phys. Lett., in press.
14. E. Yablonovitch, T. Gmitter and K. Leung, Phys. Rev. Lett. **67**, 2295 (1991).
15. C. Chan, K. Ho and C. Soukoulis, Europhys. Lett. 16, 563 (1991).
16. H. Sozüer and J. Haus, J. Optic. Soc. Am. B **10**, 296 (1993);
17. K. Ho, C. Chan, C. Soukoulis, R. Biswas and M. Sigalas, Solid State Commun. **89**, 413 (1994).
18. H. Sozüer and J. Dowling, J. Mod. Opt. **41**, 231 (1994).
19. E. Ozbay, E. Michel, G. Tuttle, M. Sigalas, R. Biswas and K. Ho, Appl. Phys. Lett. **64**, 2059 (1994).
20. S. Fan, P. Villeneuve, R. Meade and J. Joannopoulos, Appl. Phys. Lett. **65**, 1466 (1994).